## Y-cube model and fractal structure of subdimensional particles on hyperbolic lattices

Han Yan (闫寒),<sup>1,\*</sup> Kevin Slagle,<sup>2,3,4</sup> and Andriy H. Nevidomskyy<sup>1</sup>

<sup>1</sup>Department of Physics & Astronomy, Rice University, Houston, Texas 77005, USA

<sup>2</sup>Department of Electrical and Computer Engineering, Rice University, Houston, Texas 77005 USA

<sup>3</sup>Department of Physics, California Institute of Technology, Pasadena, California 91125, USA

<sup>4</sup>Institute for Quantum Information and Matter and Walter Burke Institute for Theoretical Physics,

California Institute of Technology, Pasadena, California 91125, USA

(Dated: November 30, 2022)

Unlike ordinary topological quantum phases, fracton orders are intimately dependent on the underlying lattice geometry. In this work, we study a generalization of the X-cube model, dubbed the Y-cube model, on lattices embedded in  $H_2 \times S^1$  space, i.e., a stack of hyperbolic planes. The name 'Y-cube' comes from the Y-shape of the analog of the X-cube's X-shaped vertex operator. We demonstrate that for certain hyperbolic lattice tesselations, the Y-cube model hosts a new kind of subdimensional particle, treeons, which can only move on a fractal-shaped subset of the lattice. Such an excitation only appears on hyperbolic geometries; on flat spaces treeons becomes either a lineon or a planeon. Intriguingly, we find that for certain hyperbolic tesselations, a fracton can be created by a membrane operator (as in the X-cube model) or by a fractal-shaped operator within the hyperbolic plane.

Introduction: Fracton orders [1-7] are examples of highly entangled gapped phases of matter that lie beyond the Landau-Ginzburg paradigm in that no symmetry is broken, yet they are also distinct from the more familiar topological phases of matter in that they do not possess a universal long-wavelength description in terms of a topological quantum field theory (TQFT) [8–18]. Rather, fracton orders have a nontrivial ground state degeneracy that depends not only on the topology but also on the system size [3–6] and lattice geometry [13, 19]. Furthermore, fracton orders support excitations whose mobility is restricted when we do not allow any additional excitations to be created: fractons are immobile; lineons can only move along a one-dimensional line, and planeons can only move within a two-dimensional plane [20, 21].

Much attention has been devoted to exactly solvable models that host fracton order in flat space, such as the X-cube model formulated on the cubic lattice [6]. By comparison, relatively little is known about the behavior of such models in curved spaces [22–27] (see Refs. [28–31] for works that study gapless fracton models [32–35] on curved spaces ). The fundamental motivation for introducing curvature is to investigate how it affects the properties of the fracton order, in much the same way as placing a TQFT on a manifold with a different genus teaches us about the topological nature of the ground state degeneracy. For example, it has been previously noted that curvature can lead to a robust ground state degeneracy of X-cube model even on manifolds that are topologically trivial [13]; and curvature can grant the subdimensional particles additional mobility [36, 37]. Another practical motivation for introducing curvature is to search for better error correcting fracton codes. In particular, codes on hyperbolic spaces can have favorable quantum error correcting properties [38]. It is thus interesting to examine this aspect for fracton order [39, 40].

In this Letter, we investigate a generalization of the X-cube model to the hyperbolic space  $H_2 \times S^1$ , which can be visualized as a stack of hyperbolic planes  $(H^2)$  with the top and bottom layers identified. Unlike the flat space, which only permits a small number of different lattices viewed as tessellations by regular polygons/polyhedra (i.e. the familiar square, triangular and hexagonal lattices in two dimensions), the number of distinct tessellations is infinite in hyperbolic spaces. Regular two-dimensional hyperbolic plane tessellations are enumerated by a pair of integers (p,q) satisfying  $\frac{1}{p} + \frac{1}{q} < 1/2$ , which is called the Schläfli symbol. These tessellations consist of of p-gonal regular polygons, with q polygons meeting at each vertex. Two examples of such tessellations are shown in Fig. 1.

We find that the generalized X-cube model on this hyperbolic geometry depends sensitively on the tessellation. The simplest is the case of q=4, where each vertex is locally isomorphic to that of a cubic lattice, allowing for the standard definition of the vertex operators as products of four Pauli X in each of the three locally orthogonal intersecting planes. The resulting (p,4) model has one-dimensional (1D) particles, lineons, which propagate along the geodesics of the  $H_2$  plane (as opposed to straight lines in the flat space), but otherwise are very similar to the X-cube lineons. There are nuances with the operators necessary to create individual fractons however, as we shall see below.

The most intriguing findings are for tessellations of q > 4. For even q > 4, we find new models, which we dub Y-cube (because of the Y shape of the in-plane part of two of the vertex operators in the simplest q = 6 case illustrated in Fig. 1b). Unlike the X-cube model, the Y-cube model with q > 4 does not possess lineons; instead the lineons are replaced with a new kind of quasiparticles, treeons, that can only propagate

<sup>\*</sup> hy41@rice.edu

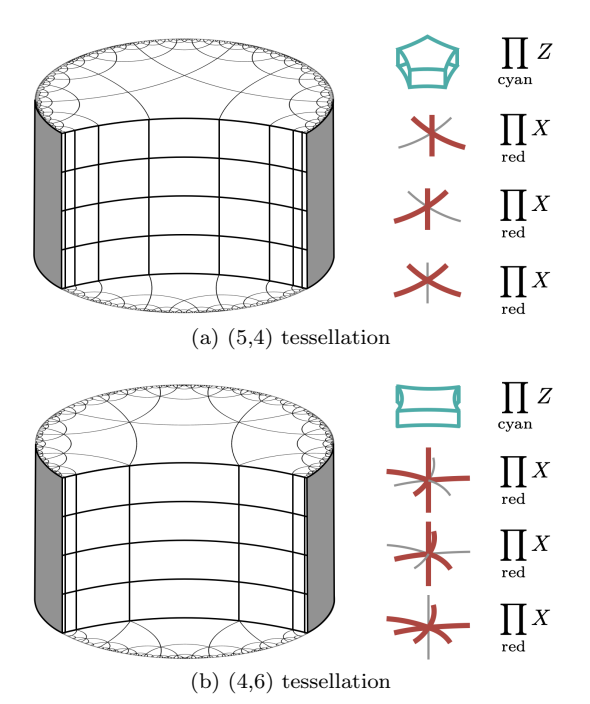


FIG. 1. Examples of tessellations of the  $H_2 \times S^1$  manifold using the Poincaré disk representation: all polygons on the disk have identical area, but look smaller when drawn farther from the center. (a) Hyperbolic tessellation with (p,q)=(5,4) (left) and Hamiltonian terms (right). (b) Hyperbolic tessellation with (p,q)=(4,6) (left) and Hamiltonian terms (right).

on a fractal tree as shown in Fig. 5b. Moreover, a pair or "dipole" of neighboring fractons remains immobile within the  $H_2$  plane, in contrast to X-cube model where fracton dipoles forms a planeon.

X-cube and Y-cube models in  $H_2 \times S^1$ : The generalized X-cube models are constructed as shown in Fig. 1. The Hamiltonian consists of two types of terms: the vertex and the prism (generalization of the cube) terms. For (p, q = 4) tessellations, the model is the natural generalization of the X-cube model [19, 36]: the vertex terms are identical to those in the X-cube model, while the "cube" terms become products of Z operators over the edges of the p-gonal prisms, as shown in Fig. 1a.

In the general case of (p,q) tessellations (with even q), we keep the p-gonal prism Z-operators in the Hamiltonian. There are in general two kinds of vertex terms: (1) a product of X operators on the two neighboring out-of-plane edges and q/2 nonadjacent in-plane edges neighboring the vertex; and (2) a product of X operators on the q in-plane edges neighboring the vertex. See Fig. 1b for a q=6 example. Each vertex term has an even number of X operators that overlap with a prism Z operators, making the model a stabilizer code Hamiltonian. We name this model the Y-cube model, alluding to the "Y" shape of the in-plane vertex terms when q=6 [Fig. 1b].

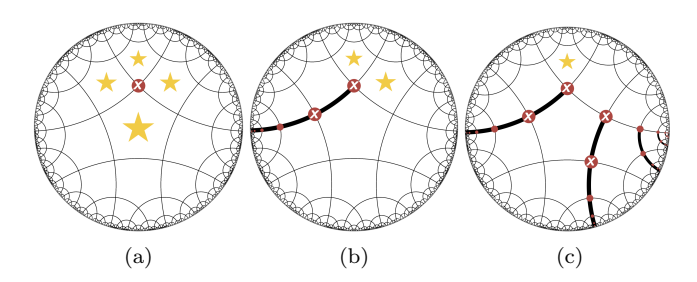


FIG. 2. Fracton operators for the (5,4) tessellation: (a) An X operator (red dot) on an out-of-plane edge (perpendicular to the shown hyperbolic plane) creates four fractons (yellow stars). (b) A truncated geodesic of X operators creates two fractons, which can move along the geodesic. (c) X operators on a stack of truncated geodesics create a single fracton.

Before we move on to describe the new features of the hyperbolic X/Y-cube models, we briefly note that all of them share some common properties due to the flat  $S^1$  dimension. Acting with an X operator on an in-plane edge will create four fracton excitations in the four prisms neighboring the edge. A pair of fractons displaced out of the plane is mobile within the hyperbolic plane (via X operators acting on the in-plane edges). A pair of fractons displaced in-plane (see e.g. Fig. 2b) is a lineon that can move in the out of plane direction. A pair of fractons displaced out of the plane is mobile within the hyperbolic plane (via Xoperators acting on the in-plane edges). Acting with a Zoperator on an out-of-plane edge will create two lineons on the two vertices at the ends of the edge. lineons are free to move in the out-of-plane direction. These excitations are similar to excitations in the cubic lattice X-cube model. However the excitations (fractons, lineons, and the new treeons) created otherwise—via X operators acting on a out-of-plane edges or Zoperators on in-plane edges—have new physics that depends on the tessellation, as we discuss in detail below.

**Fractons in** (5,4) **X-cube model:** Let us first consider the model on the hyperbolic lattice with (p,q)=(5,4) [Fig. 1a], whose physics generalizes straight-forwardly to all (odd  $p \geq 5, q=4$ ) tessellations.

We first examine the effects of an X operator acting on an out-of-plane edge. It creates four fractons (a quadrupole) on the four neighboring prisms [Fig. 2a]. By consecutively applying X operator on the out-of-plane edges attached to the same geodesic of the  $H_2$  plane, a pair (or dipole) of the fractons can be moved away. Extending one side of the string to the infinite boundary of the hyperbolic plane will leave a single pair of fractons in the bulk. Equivalently, a truncated geodesic of X operators creates a pair of fractons at its end [Fig. 2b].

Unlike in the X-cube model, a single fracton cannot be created in the bulk at the corner of a membrane operator. This is because a membrane operator creates fractons inside the membrane since each pentagon prism

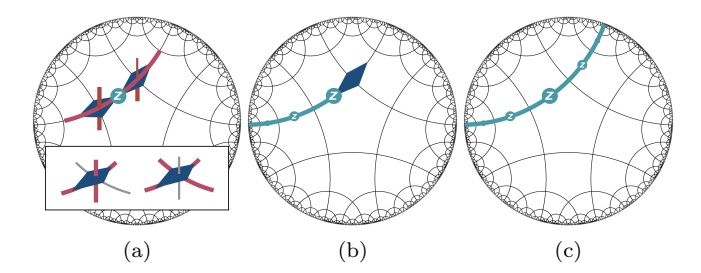


FIG. 3. Lineon operators for the (5,4) tessellation: (a) A Z operator (teal) on an in-plane edge creates two lineons (blue diamonds). The inset shows the two excited terms in the Hamiltonian for a single lineon. (b) Applying a string of Z operators along a geodesic of in-plane edges creates a single lineon, which can move along the geodesic. (c) The logical operator constructed by Z operators, which can also be viewed as moving a lineon from one boundary to the other.

is surrounded by an odd number (p=5) of out-of-plane edges. Instead, a single fracton can be created using a series of truncated geodesic strings of X operators, as illustrated in Fig. 2c. Each truncated geodesic of out-of-plane X operators creates a pair of fractons. Thus, the first truncated geodesic operator creates a pair of fractons, and the others moves one fracton in the pair away to infinity.

Lineons in (5,4) X-cube model: Next we examine the action of Z operators on in-plane edges. When q=4, each vertex is locally identical to a vertex of the cubic lattice. Hence, a Z operator on an in-plane link creates two lineons [Fig. 3a] that behave similarly to lineons in the X-cube model on a cubic lattice. Each lineon is an excited state of two vertex operators, shown in the inset of Fig. 3a. Lineons are restricted to move on a  $H_2$  geodesic, as shown in Fig. 3b. Under rough boundary conditions (which condense lineons) of the hyperbolic planes, the product of Z operators along a geodesic [Fig. 3c] becomes a logical operator that does not create any excitations.

Fractors in (4,6) Y-cube model: Next we consider the Y-cube model on (even  $p \geq 4, q \geq 6$ ) tessellations. We find that  $q \geq 6$  results in novel physics with a new kind of restricted particle mobility. We focus on the representative example of (4,6), with the Hamiltonian shown in Fig. 1b. We first discuss the properties of fractors, then we consider the treeons (which are analogs of lineons).

On the (4,6) tessellation, there are two ways to create fractons, illustrated in Fig. 4. To understand the first way, it is helpful to first construct logical out-of-plane X operators that do not create any fractons in the bulk, shown in Fig. 4a. The logical operator is a product of X operators on a fractal tree (also known as a Bruahat-Tits tree). The fractal tree is constructed by choosing q/2 non-adjacent edges at a vertex and repeating this

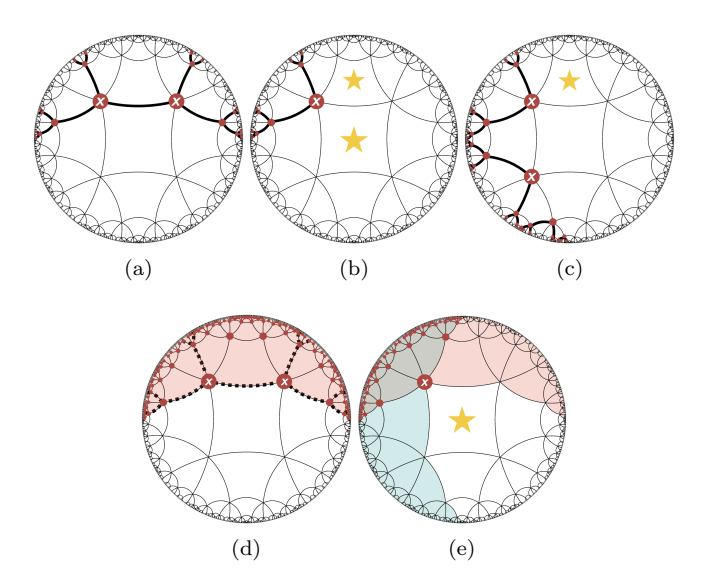


FIG. 4. Fracton operators for the (4,5) tessellation: (a) A bulk logical X operator on a fractal tree (thick black), which is a product of X operators (red dots) on out-of-plane edges neighboring one (out-of-plane) side of the fractal tree. (b) A pruned fractal-tree of X operators creates a pair of fractons, which is a lineon with mobility only in the out-of-plane direction. (c) An infinite series of the pruned fractal-trees creates a single fracton. (d) A bulk logical X operator on a fractal tree wedge (colored red). It is the product of all X operators (red dots) on the out-of-plane edges neighboring one side of the wedge. The fractal tree is drawn in thick, dashed line. (e) A membrane of X operators supported on the intersection of two wedges (red and teal) also creates a single fracton.

procedure at every vertex it extends to. We shall refer to these logical operators as  $T_X$ . The  $T_X$  operators anticommute with strings of Z operators in the out-of-plane direction. Here, we assume either an infinite hyperbolic plane or a finite plane with a boundary that condenses fracton dipoles [41, 42].

Now we can see how single fracton and fracton dipoles are created by the first type of fractal tree operator: an in-plane fracton dipole is created by pruning the fractal tree operator  $T_X$  at a vertex in the bulk, as shown in Fig. 4b. Unlike the X-cube model on a cubic lattice or a (p,q=4) tessellation, for even  $q\geq 6$  the in-plane fracton dipoles are lineons that can only move in the out-of-plane direction. A single fracton can be created by aligning many pruned fractal trees along a series of adjacent vertices, as shown in Fig. 4c. Each pruned tree, creating a dipole, serves the purpose of moving a fracton closer to the boundary.

Now we turn to a second type of fracton-creation operator. Recall that when p is odd (such as p=5 in the earlier example in Fig. 2), a membrane of X operators creates an extensive number of excitations because each prism term overlaps with the membrane operate by an odd number (p) of out-of-plane edges. However when p is even, X membrane operators commute with the prism

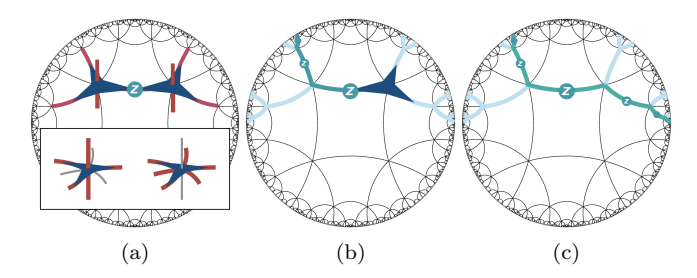


FIG. 5. Tree on operators for the (6,4) tessellation: (a) A Z operator (teal) on an in-plane edge creates two tree ons (blue stars). The inset shows the two excited terms in the Hamiltonian for a single tree on. (b) Applying a string of Z operators (colored teal) within the fractal tree (colored light teal) creates a single tree on. The tree on can only move within the fractal tree. (c) An infinite string of Z operators within the fractal tree is a logical operator.

term in the bulk.

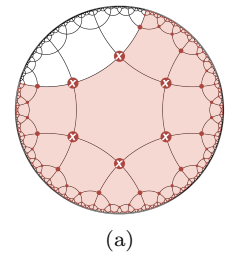
The key to constructing such membrane operators is that its boundary should overlap with the neighbouring prisms by two out-of-plane edges. Following this principle, the membrane boundary should follow this pattern: we first find a q/2-degree fractal tree we constructed earlier. Then, we select a region bounded by the branches of the tree that contains the entire tree [shaded region in Fig. 4d]. The membrane operator is the product of all the X operators on the out-of-plane edges attached to this region (on the top or bottom side of the  $H^2$  plane). We name this geometric shape the fractal-tree wedge.

To construct a membrane operator that creates a single fracton, we can select two partially overlapping fractal-tree wedges. The membrane operator supported on the overlap creates a single fracton near the intersection of wedge boundaries, as shown in Fig. 4e.

Treeons in (4,6) Y-cube model: Let us now discuss the excitations that result from Z operators acting on the in-plane edges in the (4,6) Y-cube model. A single in-plane Z operator creates two composite excitations, each consisting of two excited vertex operators, as shown in Fig. 5a. The two excited vertex operators (inset of Fig. 5a) share three in-plane edges. Acting with a Z operator on one of these shared edges will move the composite excitation to the adjacent vertex on the other side of the edge. The excitation cannot move along other edges without creating additional excitations.

Repeating this procedure, we find that this composite excitation can move anywhere on the fractal tree shown in Fig. 5b. The construction of such a tree is the same as  $T_X$  in Fig. 4a. This composite excitation is similar to a lineon, except at each vertex it can choose between multiple fractal paths. We call this new kind of mobility-restricted excitation a treeon since its mobility is restricted to a fractal tree.

One non-trivial consequence of the treeons is how they form logical operators. A treeon can travel from any one



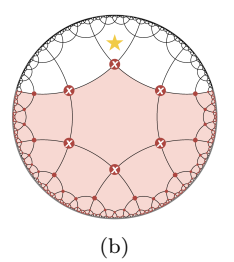


FIG. 6. (a) A logical membrane X operator as the geodesic wedge for the (6,4) model. (b) A membrane X operator with a corner that creates a fraction.

of the many branches of the tree to any other one. The product of the Z operators along any such path is then a logical operator (assuming rough boundary conditions that condense treeons). One example is shown in Fig. 5c.

Generalization to all tessellations: Let us now summarize some properties of the hyperbolic X/Y-cube models on all (p,q) tessellations with even q. When  $q \geq 6$ , X-cube lineons are replaced by a new type of excitations, treeons, that move on the fractal tree. The q=4 case can be viewed as a special limit of a tree with only two branches at each vertex, which becomes a geodesic. In this limit the treeons become lineons, and fracton dipoles gain mobility along the geodesics. The properties of different hyperbolic lattices are summarized in Table. I.

When p is odd, a fracton can be created at the end of a series of truncated geodesics or fractal trees [Figs. 4c,2c]. When p is even, logical X membrane operators are allowed in the shape of fractal-tree wedges for  $q \geq 6$  [Fig. 4e] or geodesic wedges for q = 4 [Fig. 6a]. The intersection of two of these logical operators creates a single fractons at the corner [Figs. 4e and 6b].

Finally, tessellations of 1/p+1/q=1/2 are special limits of the embedding space becoming flat rather than hyperbolic. In the case of p=q=4 (square lattice) we recover the 3D X-cube model on a cubic lattice. When (p=3,q=6), the 2D tessellation forms a triangular lattice, and we can define the Y-cube model on a stack of these triangular lattices. In this case, the Y-cube model treeons we encountered for (p>3,q=6) become planeons that move on a honeycomb network embedded in the flat triangular layer. This results because when the hyperbolic geometry is made flat, the fractal tree that the treeon can traverse collapses onto itself and reduces to a 2D honeycomb, see the Supplementary Materials for more detail (although we leave the in-depth study of this triangular model to future work).

Summary and outlook: We introduced the Y-cube model on stacked tessellations of the hyperbolic plane. We discovered that the Y-cube model features a new kind of particle with restricted mobility: a treeon, which is constrained to move along a fractal tree. We also find

lattice and model	$\begin{array}{c} \text{in-plane} \\ \text{lineon/treeon} \end{array}$	in-plane fracton dipole	in-plane $X$ logical op.	in-plane fracton creation op.
(p  odd, q = 4)  X-cube	lineon, Fig. 3b	1D mobility, Fig. 2b	geodesic	truncated geodesics, Fig. 2b
(p  even, q = 4)  X-cube	lineon	1D mobility	geodesic, geodesic wedge, Fig. 6a	truncated geodesics, wedge corner, Fig. 6b
$(p \text{ odd}, q \ge 6) \text{ Y-cube}$	treeon	no mobility	fractal tree	pruned fractal trees
$(p \text{ even}, q \ge 6) \text{ Y-cube}$	treeon, Fig. 5b	no mobility, Fig. 4b	fractal tree, Fig. 4a, fractal-tree wedge, Fig. 4d	pruned fractal trees, Fig. 4c, wedge corner, Fig. 4e

TABLE I. Properties of hyperbolic X/Y-cube models on different tessellations of  $H_2 \times S^1$ 

that in the hyperbolic X-cube and Y-cube models with even p, fractons can be created by either in-plane membrane or fractal operators (Figs. 4c and 4). We are not aware of any previously studied models with this property.

These models also serve as a concrete example of how the lattice geometry (tessellation) of fracton orders can determine their fundamental properties, even when the embedding space (in this case  $H_2 \times S^1$ ) is the same. Our discovery suggests that there are still many fracton orders with new and exotic features not seen before, especially when their underlying graphs/lattices are beyond the flat space ones, i.e., lattices with no translational symmetry. Like Type-II fracton orders, the hyperbolic Y-cube models are not foliated fracton orders [19, 43], challenging us for new insight of classification schemes of fracton order [44].

This work provides one of the simplest examples of fracton order beyond the flat space, but there is much room left for future exploration. One future topic is to impose boundary conditions on the hyperbolic plane and study the ground state degeneracy, logical operators, and quantum information encoding. It is also useful to ask if the new physics from the hyperbolic structure provides benefits in quantum memory storage. Another direction is to investigate fracton models on the 3D hyperbolic space  $H_3$ , or general graphs without translational symmetry [25].

H.Y. and A.H.N. were supported by the National Science Foundation Division of Materials Research under the Award DMR-1917511. K.S. was partially supported by the Walter Burke Institute for Theoretical Physics at Caltech; and the U.S. Department of Energy, Office of Science, National Quantum Information Science Research Centers, Quantum Science Center.

M. Pretko, X. Chen, and Y. You, Int. J. Mod. Phys. A 35, 2030003 (2020), publisher: World Scientific Publishing Co.

<sup>[2]</sup> R. M. Nandkishore and M. Hermele, Annual Review of Condensed Matter Physics 10, 295 (2019), arXiv:1803.11196.

<sup>[3]</sup> S. Bravyi, B. Leemhuis, and B. M. Terhal, Annals of Physics 326, 839 (2011), arXiv:1006.4871.

<sup>[4]</sup> J. Haah, Phys. Rev. A 83, 042330 (2011), publisher: American Physical Society.

<sup>[5]</sup> S. Vijay, J. Haah, and L. Fu, Phys. Rev. B 92, 235136 (2015).

<sup>[6]</sup> S. Vijay, J. Haah, and L. Fu, Phys. Rev. B 94, 235157 (2016).

<sup>[7]</sup> C. Chamon, Phys. Rev. Lett. **94**, 040402 (2005).

<sup>[8]</sup> N. Seiberg and S.-H. Shao, SciPost Phys. 10, 3 (2021), arXiv:2004.06115.

<sup>[9]</sup> P. Gorantla, H. T. Lam, N. Seiberg, and S.-H. Shao, Phys. Rev. B 104, 235116 (2021), arXiv:2108.00020.

<sup>[10]</sup> K. Slagle, Phys. Rev. Lett. 126, 101603 (2021), arXiv:2008.03852.

<sup>[11]</sup> K. Ohmori and S. Shimamura, arXiv e-prints (2022), arXiv:2210.11001.

<sup>[12]</sup> W. Fontana, P. Gomes, and C. Chamon, SciPost Physics

<sup>12, 064 (2022),</sup> arXiv:2103.02713.

<sup>[13]</sup> K. Slagle and Y. B. Kim, Phys. Rev. B 96, 195139 (2017).

<sup>[14]</sup> D. Aasen, D. Bulmash, A. Prem, K. Slagle, and D. J. Williamson, Phys. Rev. Research 2, 043165 (2020), arXiv:2002.05166.

<sup>[15]</sup> X.-G. Wen, Phys. Rev. Research 2, 033300 (2020), arXiv:2002.02433.

<sup>[16]</sup> J. Wang, "Non-Liquid Cellular States," (2020), arXiv:2002.12932.

<sup>[17]</sup> K. Slagle, D. Aasen, and D. Williamson, SciPost Physics 6, 043 (2019), arXiv:1812.01613.

<sup>[18]</sup> M. Qi, L. Radzihovsky, and M. Hermele, Annals of Physics 424, 168360 (2021), arXiv:2010.02254 [condmat.str-el].

<sup>[19]</sup> W. Shirley, K. Slagle, Z. Wang, and X. Chen, Phys. Rev. X 8, 031051 (2018), arXiv:1712.05892.

<sup>[20]</sup> S. Pai and M. Hermele, Phys. Rev. B 100, 195136 (2019), arXiv:1903.11625.

<sup>[21]</sup> M.-Y. Li and P. Ye, Phys. Rev. B 101, 245134 (2020), arXiv:1909.02814 [cond-mat.str-el].

<sup>[22]</sup> H. Yan, Phys. Rev. B 99, 155126 (2019), arXiv:1807.05942 [hep-th].

<sup>[23]</sup> H. Yan, Phys. Rev. B 100, 245138 (2019).

<sup>[24]</sup> H. Yan, Phys. Rev. B **102**, 161119 (2020).

- [25] P. Gorantla, H. Tat Lam, and S.-H. Shao, arXiv e-prints (2022), arXiv:2207.08585.
- [26] P. Gorantla, H. Tat Lam, N. Seiberg, and S.-H. Shao, arXiv e-prints, arXiv:2210.03727 (2022), arXiv:2210.03727 [cond-mat.str-el].
- [27] D. Radicevic, arXiv e-prints (2019), arXiv:1910.06336.
- [28] K. Slagle, A. Prem, and M. Pretko, Annals of Physics 410, 167910 (2019), arXiv: 1807.00827.
- [29] L. Bidussi, J. Hartong, E. Have, J. Musaeus, and S. Prohazka, SciPost Physics 12, 205 (2022), arXiv:2111.03668 [hep-th].
- [30] A. Jain and K. Jensen, SciPost Phys. 12, 142 (2022).
- [31] A. Gromov, Phys. Rev. Lett. 122, 076403 (2019), arXiv:1712.06600.
- [32] M. Pretko, Phys. Rev. B **95**, 115139 (2017).
- [33] N. Seiberg and S.-H. Shao, SciPost Physics 9, 046 (2020), arXiv:2004.00015.
- [34] M. Pretko and L. Radzihovsky, Phys. Rev. Lett. 120, 195301 (2018), arXiv:1711.11044.
- [35] X. Chen, H. T. Lam, and X. Ma, arXiv e-prints , arXiv:2211.10458 (2022), arXiv:2211.10458 [cond-mat.str-el].
- [36] K. Slagle and Y. B. Kim, Phys. Rev. B 97, 165106 (2018), arXiv:1712.04511.
- [37] K. Slagle, A. Prem, and M. Pretko, Annals of Physics 410, 167910 (2019), arXiv:1807.00827.
- [38] N. P. Breuckmann and J. N. Eberhardt, IEEE Transactions on Information Theory 67, 6653 (2021), arXiv:2012.09271.
- [39] K. T. Tian, E. Samperton, and Z. Wang, Annals of Physics 412, 168014 (2020), arXiv:1812.02101.
- [40] K. T. Tian and Z. Wang, arXiv e-prints (2019), arXiv:1902.04543.
- [41] D. Bulmash and T. Iadecola, Phys. Rev. B 99, 125132 (2019), arXiv:1810.00012.
- [42] Z.-X. Luo, R. C. Spieler, H.-Y. Sun, and A. Karch, Phys. Rev. B 106, 195102 (2022).
- [43] W. Shirley, K. Slagle, and X. Chen, SciPost Phys. 6, 015 (2019), arXiv:1803.10426.
- [44] A. Dua, P. Sarkar, D. J. Williamson, and M. Cheng, Physical Review Research 2, 033021 (2020), arXiv:1909.12304 [cond-mat.str-el].
- [45] X. Chen, Z.-C. Gu, and X.-G. Wen, Phys. Rev. B 82, 155138 (2010), arXiv:1004.3835.
- [46] N. Tantivasadakarn, W. Ji, and S. Vijay, Phys. Rev. B 103, 245136 (2021), arXiv:2102.09555.

## Supplementary Materials for "Y-cube model and fractal structure of subdimensional particles on hyperbolic lattices"

## I. THE CASE OF (3,6) TESSELLATION

Here, we discuss some properties of the Y-cube model on the (3,6) tessellation (triangular lattice)  $\times S^1$ . This is a special limit of the (p,q) tessellations that is geometrically flat instead of hyperbolic, which drastically affects the mobility properties of the excitations. We leave a more complete study of this model to future work.

The Hamiltonian consists of three types of terms, shown in Fig. S1. The first two types are the product of Z's on the edges of a triangle prism, and certain products of X's around vertices. On this flat tessellation, an additional term can be added to the Hamiltonian, which is not analogous to any term in hyperbolic tessellations: namely the product of Z's around a hexagon. The existence of this third term only on flat space is related to the fact (explained below) that Z operators on in-plane edges create planons, rather than treeons as in the hyperbolic Y-cube model.

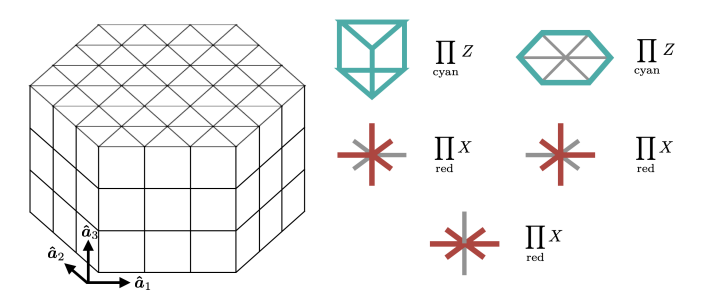


FIG. S1. The triangular  $\times S^1$  lattice and its Hamiltonian terms.

We first examine the excited states of the vertex terms. Recall from the main text that when p > 3 and q = 6, Z operators acting on in-plane edges create treeon excitations that are restricted to move on a fractal tree. However on the (3,6) tessellation, we find that these vertex excitations are instead planeons. This can be seen as follows. Locally, a Z operator on an in-plane edge creates two such planeons [Fig. S2a]. Each planeon is in the excited state of two vertex operators [inset of Fig. S2a]. Similar to a treeon, these planeons can move along any one of three in-plane edges connected to its vertex. However since the lattice is no longer hyperbolic, this mobility results in the mobility of a planeon, which can move within a hexgonal sublattice, as shown in Fig. S2b. There are three flavors of this planeon, one flavor for each hexagonal sublattice. The flavor of the planeon can be changed at the expense of creating the fully mobile excitation described in the following paragraph.

In hyperbolic geometry, the composite excited state of two vertex operators created by an out-of-plane Z oper-

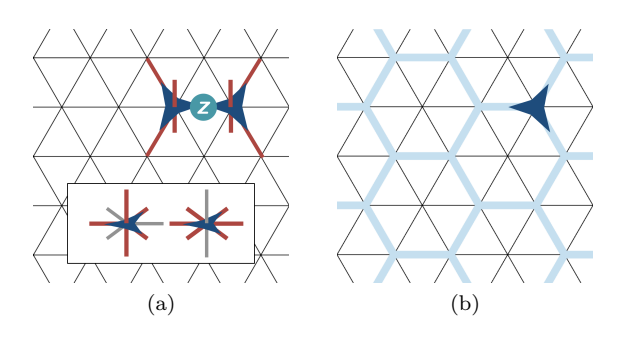


FIG. S2. (a) A Z operator (teal) acting on an in-plane edge creates two planeons (blue stars). The inset shows the two excited terms in the Hamiltonian for a single planeon. (b) A single planeon can travel on the hexagonal sublattice of the triangular lattice, colored in light blue.

ator is a lineon that can move in the vertical direction only. On the (3,6) tessellation, the analogous excitation is instead free to move in 3D. Three Z operators on the edges of an in-plane triangle creates three such excitations [Fig. S3a]. Each composite excitation is in the excited state of two vertex operators [inset of Fig. S3a]. Unlike on the hyperbolic plane, the flat geometry allows these composite excitations to move along six in-plane directions, as shown in Fig. S3b. Repeated in-plane movement can span a triangular sub-lattice on the original lattice. These composite excitations can also move along the vertical direction as shown in Fig. S3c, giving them 3D mobility.

These composite vertex excitations are similar to 3D toric code charges. Naively, there are three flavors: one on each of the 3 sublattices. But by acting with a triangle of Z operators [Fig. S3a], the composite of three flavors annihilate. Thus, there are actually only two independent flavors. The corresponding flux operator (similar to a 3D toric code flux operator) is the membrane operator consisting of an out-of-plane stack of products of X operators on the red links in Fig. S4. This 2D membrane operator creates a loop excitation around its boundary. Presumably, there are two flavors of this membrane operator.

The action of in-plane X operators creates planeon excitations with in-plane mobility. The planeon is a composite excitations of the Z terms shown in Fig. S5. This planeon anticommutes with the planeon shown in Fig. S2.

Finally, we note that for an  $L \times L \times L$  periodic lattice (with lattice constants  $\hat{a}_{1,2,3}$  shown in Fig. S1), the ground state degeneracy is GSD =  $2^{6+2L}$  when L is multiple of 3 (for which different flavors of particles do not turn into each other due to boundary conditions).

Therefore, this model supports a pair of anticommut-

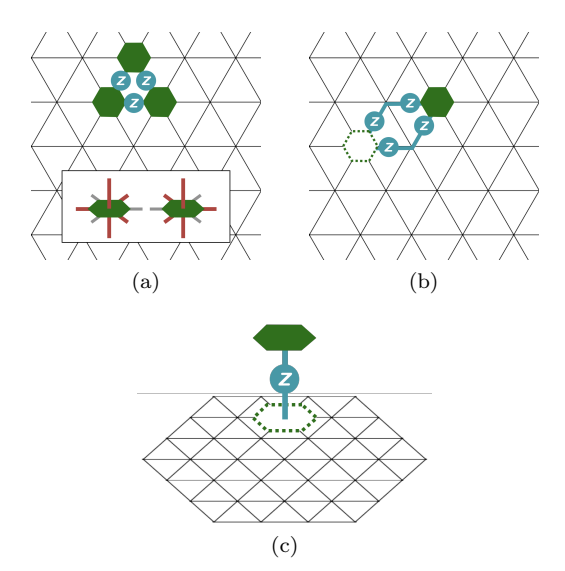


FIG. S3. (a) Three Z operators (teal) acting on an in-plane triangle creates three excitations (green hexagons). The inset shows the two excited terms in the Hamiltonian for a single excitation. (b) A single excitation can travel on a sub-triangular lattice of the original triangular lattice. This movement is done using four Z operators shown on the figure. (c) A single excitation can also travel vertically. This movement is done using a Z operator on the vertical link shown on the figure.

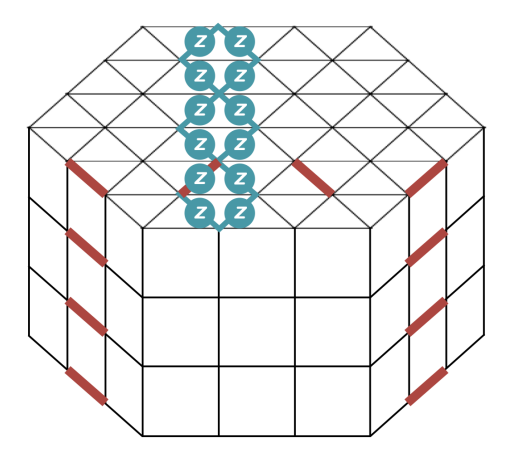


FIG. S4. A flux operator consisting of a product of X operators (red) within a 2D membrane. The flux operator anticommutes with the string operator (Fig. S3b) of the mobile charge excitation.

ing planeons on each layer, similar to stacks of toric code. The model also supports two sets of fully mobile charges along with flux-line excitations, similar to two copies of 3D toric code. Thus, it seems plausible that the model is local-unitary equivalent [45] to the following hybrid fracton order [46]: two copies of 3D toric code and decoupled stacks of 2D toric codes. Indeed, the ground state degeneracy is also consistent with this possibility. We leave the resolution of this possibility to future work.

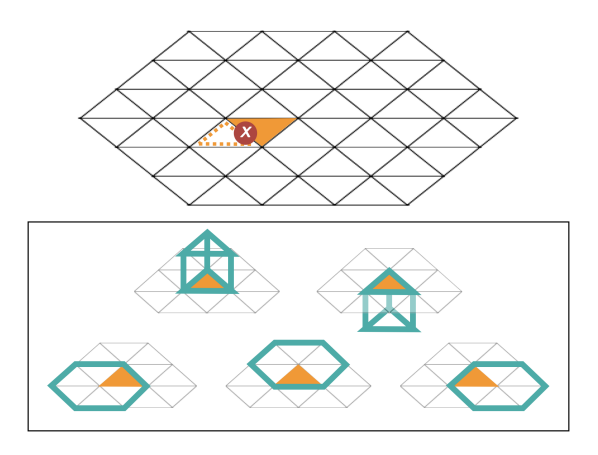


FIG. S5. The action of an in-plane X operator moves a planeon (orange triangle in the top panel). The planeon is a composite excitations of the five Z terms (teal) shown in the lower panel.